The Canadian Mineralogist
Vol. 43, pp. 759-767 (2005)

RIETVELD REFINEMENT OF SYNTHETIC MONOCLINIC $NaBSiO_4$

HERIBERT A. GRAETSCH[§] AND WERNER SCHREYER

Institut für Geologie, Mineralogie und Geophysik, Ruhr-Universität Bochum, D–44780 Bochum, Germany

ABSTRACT

A full-pattern X-ray powder-diffraction refinement reveals that $NaBSiO_4$ prepared at 6 GPa and 700°C crystallizes in space group $P2_1/n$ with the structure of beryllonite, $NaBePO_4$. With a 7.9845(5), b 7.6969(5), c 13.9432(9) Å, β 90.081(6)° and V 856.89(2) Å^3, $NaBSiO_4$ has the smallest unit-cell volume of all known compounds with the beryllonite structure. A naturally occurring counterpart could be the unnamed mineral UK53 from Mont Saint-Hilaire, Quebec, Canada. The crystal structure of monoclinic $NaBSiO_4$ is closely related to that of the hexagonal mineral malinkoite, with the same chemical composition. The structural differences are mainly caused by variant arrangements of two kinds of six-membered rings made up of alternating (BO_4) and (SiO_4) tetrahedra.

Keywords: beryllonite, synthetic $NaBSiO_4$, malinkoite, stuffed tridymite.

SOMMAIRE

Un affinement du spectre de poudre entier en diffraction X du composé $NaBSiO_4$, synthétisé à 6 GPa et 700°C, a montré qu'il cristallise dans le groupe d'espace $P2_1/n$ avec la structure de la béryllonite ($NaBePO_4$). Avec les paramètres de maille a 7.9845(5), b 7.6969(5), c 13.9432(9) Å, β 90.081(6)° et V 856.89(2) Å^3, le $NaBSiO_4$ possède la maille la plus petite de tous les composés à structure de type béryllonite. Un analogue naturel pourrait être le minéral sans nom UK53 de Mont Saint-Hilaire, au Québec. La structure cristalline de notre composé monoclinique est intimement liée à celle de la malinkoïte, hexagonale, dont la composition est aussi $NaBSiO_4$. Les différences structurales sont essentiellement dues aux divers arrangements des deux types d'anneaux à six membres constitués d'une alternance de tétraèdres (BO_4) et (SiO_4).

Mots-clés: béryllonite, composé $NaBSiO_4$, malinkoïte, tridymite insérée.

INTRODUCTION

In 1996, M. Ufer, in the course of his Diploma Thesis at this Institute, performed an experimental study on the synthesis and stability of reedmergnerite (the boron analogue of albite) and showed that H_2O-free $NaBSi_3O_8$ decomposes at pressures in excess of about 3.5 GPa and 450–800°C to coesite and an unknown $NaBSiO_4$ phase (Ufer & Schreyer 1996, Werding & Schreyer 1996, Schreyer & Werding 1997). Scanning electron microscopy of this phase revealed platy euhedral crystals with apparently hexagonal morphology measuring about one micrometer in diameter with a thickness of less than 0.5 micrometer (Ufer 1996). As a result of six electron-microprobe analyses for Na and Si, no significant deviations from the stoichiometry $NaBSiO_4$ were detected.

Since the $NaBSiO_4$ phase first synthesized by Ufer (1996) had been insufficiently characterized, a sample provided by M. Ufer was studied in the present investigation by X-ray powder diffraction. The density calculated from the new data (2.926 g/cm^3), its monoclinic symmetry ($P2_1/n$) and the strongest six X-ray powder reflections approximately coincide with those reported by Chao *et al.* (1990) for an unnamed $NaBSiO_4$ mineral from Mont Saint-Hilaire, Quebec, labeled UK53.

Recently, Sokolova *et al.* (2001) described the crystal structure of malinkoite from the Kola Peninsula, which also has the formula $NaBSiO_4$. It has a hexagonal symmetry and, following a personal communication with E. Sokolova (2004), is equivalent to the unnamed hexagonal $NaBSiO_4$ mineral from Mont Saint-Hilaire labeled UK53A by Chao *et al.* (1990). To complicate matters, there is still another hexagonal $NaBSiO_4$ mineral from Mont Saint-Hilaire, labeled UK53B by Wight & Chao (1995). Thus, rather complicated polymorphic relations may exist for the stoichiometry $NaBSiO_4$.

[§] *E-mail address*: heribert.graetsch@rub.de

Experimental Details

Sample preparation

Ufer (1996) synthesized his $NaBSiO_4$ phase from a stoichiometric mixture of sodium tetraborate and aerosil (synthetic highly dispersed silica produced by high-temperature hydrolysis, provided by Degussa AG) in a high-pressure piston–cylinder apparatus at 4.0 GPa and 750°C. In order to test for possible instability of the phase at still higher pressure, he reran the material at 6.0 GPa and 700°C, but found no change. This sample was used in the present study. No further chemical analyses were carried out as only a small amount of material was available. The sample was ground in a boron carbide mortar and loaded into a glass capillary with a diameter of 0.3 mm.

X-ray powder diffraction

An X-ray powder diffractogram was recorded on a Siemens D5000 diffractometer operating in Debye–Scherrer configuration. Copper $K\alpha_1$ radiation was selected with a focusing Ge monochromator. The sample was rotated during the measurement. The reflections were recorded with a 5° wide position-sensitive detector. Six scans ranging from 8 to 95°2θ with a step size of 0.0078° were added in order to yield a single dataset. The total counting time was 65 hours for 11154 steps. The powder diffractogram could be indexed with monoclinic symmetry, yielding lattice parameters close to those reported by Chao *et al.* (1990) for the unnamed $NaBSiO_4$ mineral UK53.

Refinement

A full-pattern Rietveld refinement was carried out with the program Jana2000 (Petricek & Dusek 2003). Initially, zero shift, background, profile and lattice parameters were refined without any structural model according to the LeBail method (LeBail *et al.* 1988). The background is high and complicated, mainly owing to diffuse intensity from the glass capillary; it was fitted with a Legendre polynomial using 24 terms. The extinctions are consistent with the space group $P2_1/n$; however, a few weak reflections indicated the admixture of small amounts of some additional phases, of which gold and coesite could be identified. The gold presumably stems from the capsule used for the high-pressure experiment. Its reflections could readily be identified owing to their broadness, which is presumably caused by microstrain introduced during the high-pressure experiment. The origin of two further very weak additional reflections (relative intensity less than 0.8%) could not be determined with certainty. Therefore, the corresponding ranges from 26.53 to 26.94° and from 27.27 to 27.52° 2θ were excluded from further refinements (Fig. 1).

The structure refinement was started with the atom coordinates of beryllonite, $NaBePO_4$, according to Golovastikov (1962), but replacing the atomic form factors of B for those of Be, and those of Si for those of P. Constraints were set so that the Si–O distances remained close to 1.620(1) Å, and the B–O distances, close to 1.470(1) Å, as reported for malinkoite (Sokolova *et al.* 2001). The O–T–O tetrahedron angles were constrained to remain close to 109.5(2)°. The refinement converged rapidly, confirming the correctness of the chosen structural model. A scale factor and a single overall atomic displacement parameter were refined for $NaBSiO_4$, coesite and gold. The positional parameters of atoms in coesite and gold were not refined. The mass fractions refined to 94.7(4) $NaBSiO_4$, 4.0(4) coesite and 1.32(8) wt.% gold. In the final stages of the refinement, all 109 parameters (including 63 positional parameters for $NaBSiO_4$) were varied simultaneously. The *R* values are listed in Table 1. A difference-Fourier synthesis did not show residual maxima larger than 0.5 e/Å^3. The uncertainties associated with the atom coordinates are multiplied by a Brerar factor of 4.703, as provided by the Jana2000 program package in order to account for possible serial correlations, which could lead to unrealistically small values of the estimated standard deviations.

No absorption correction was carried out. Texture effects were not observed. Refinement of individual displacement-parameters of the atoms led to unreasonable

TABLE 1. EXPERIMENTAL AND REFINEMENT DETAILS

Chemical formula	$NaBSiO_4$
Space group	$P2_1/n$
Unit-cell dimensions	
a (Å)	7.9845(6)
b (Å)	7.6969(6)
c (Å)	13.9432(10)
β (°)	90.081(7)
V (Å^3)	856.891(15)
Formula units per unit cell	12
Calculated density	2.9264(5) g/cm^3
F(000)	744
Diffractometer	Siemens D5000
Monochromator	Ge(111)
Radiation	Cu$K\alpha_1$
2 θ (°)	8.000 - 94.659
Increment (°)	0.008
Excluded regions (°)	26.527 - 26.940, 27.271 - 27.519
Profile function	Pseudo-Voigt
Background function	24 Legendre polynomials
Weighting scheme	Sigma
Phase volume, in %	
$NaBSiO_4$	95.7(4)
Coesite	4.1(4)
Gold	0.20(2)
Number of data points	11069
Number of refined parameters	109
Profile *R*	0.0522
Profile *wR*	0.0770
Profile *wR* expected	0.0190
Goodness of fit	4.06
Number of reflections	780
Bragg	
R(obs)	0.0489
wR(obs)	0.0572
R(all)	0.0491

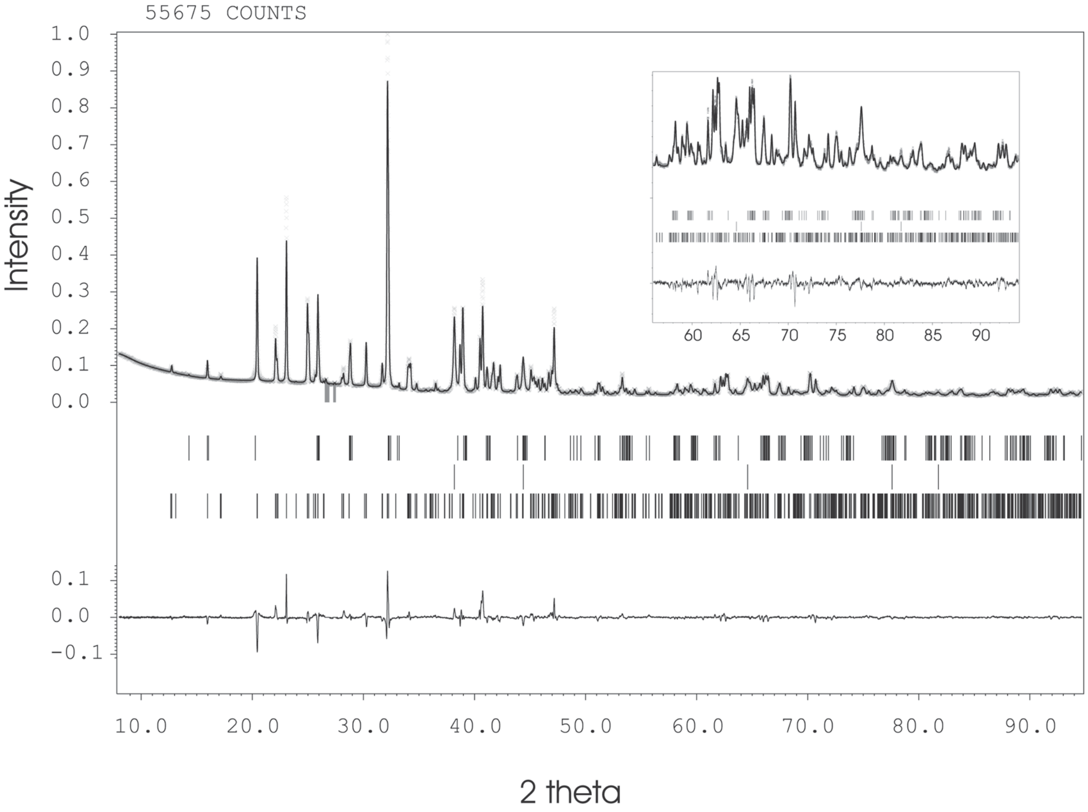

FIG. 1. Calculated and observed (crosses) X-ray powder diffractogram of synthetic monoclinic $NaBSiO_4$. The difference (observed – calculated) is plotted below. The short vertical bars indicate the position of the reflections. First row: coesite (4.0 wt.%), second row: gold (1.3 wt.%), third row: $NaBSiO_4$ (94.7 wt.%).

differences among the oxygen atoms, and the results were discarded in spite of the lower *R*-values obtained. Interchange of B and Si resulted in much higher *R*-values, supporting the validity of the initially assumed distribution of cations. Reduction of the weights on the distance constraints yielded lower *R*-values, but also a physically implausible large spread among the Si–O and B–O distances, leaving the average values unchanged.

STRUCTURE DESCRIPTION AND COMPARISON TO MALINKOITE

The framework of tetrahedra

Monoclinic $NaBSiO_4$ synthesized at high pressure is isotypic with beryllonite, $NaBePO_4$. The B^{3+} ion (*r* 0.11 Å) replaces Be^{2+} (*r* 0.27 Å), and Si^{4+} (*r* 0.27 Å) substitutes for P^{5+} (*r* 0.17 Å) (Shannon 1976) at the tetrahedral sites in spite of the reverse size-ratio of the cations. The atom coordinates are listed in Table 2. The crystal structure of synthetic monoclinic $NaBSiO_4$ is closely related to that of the hexagonal mineral malinkoite from the Kola Peninsula, Russia, which has the same chemical composition (Sokolova *et al.* 2001). There is, however, no group–subgroup relationship between the polymorphs ($P2_1/n$ and $P6_3$, respectively).

In tridymite and its stuffed derivatives, corner sharing of the tetrahedra result in a three-dimensional framework in which the tetrahedra form layers made up of six-membered rings. However, the layers of six-membered rings are stacked in a different way in the various stuffed derivatives. Whereas adjacent layers are mirror images of each other in high-temperature tridymite, they are additionally rotated by 180° around their perpendicular axis in beryllonite, malinkoite and kalsilite ($KAlSiO_4$), and shifted laterally. These modifications result in a different arrangement of the tetrahedra, which is most easily seen when viewed along the axis perpendicular to the layers. The eclipsed or *cis* configuration in tridymite and nepheline ($Na_{1-x}K_xAlSiO_4$) contrasts with staggered or *trans* configuration in beryllonite, malinkoite and kalsilite. Furthermore, tridymite,

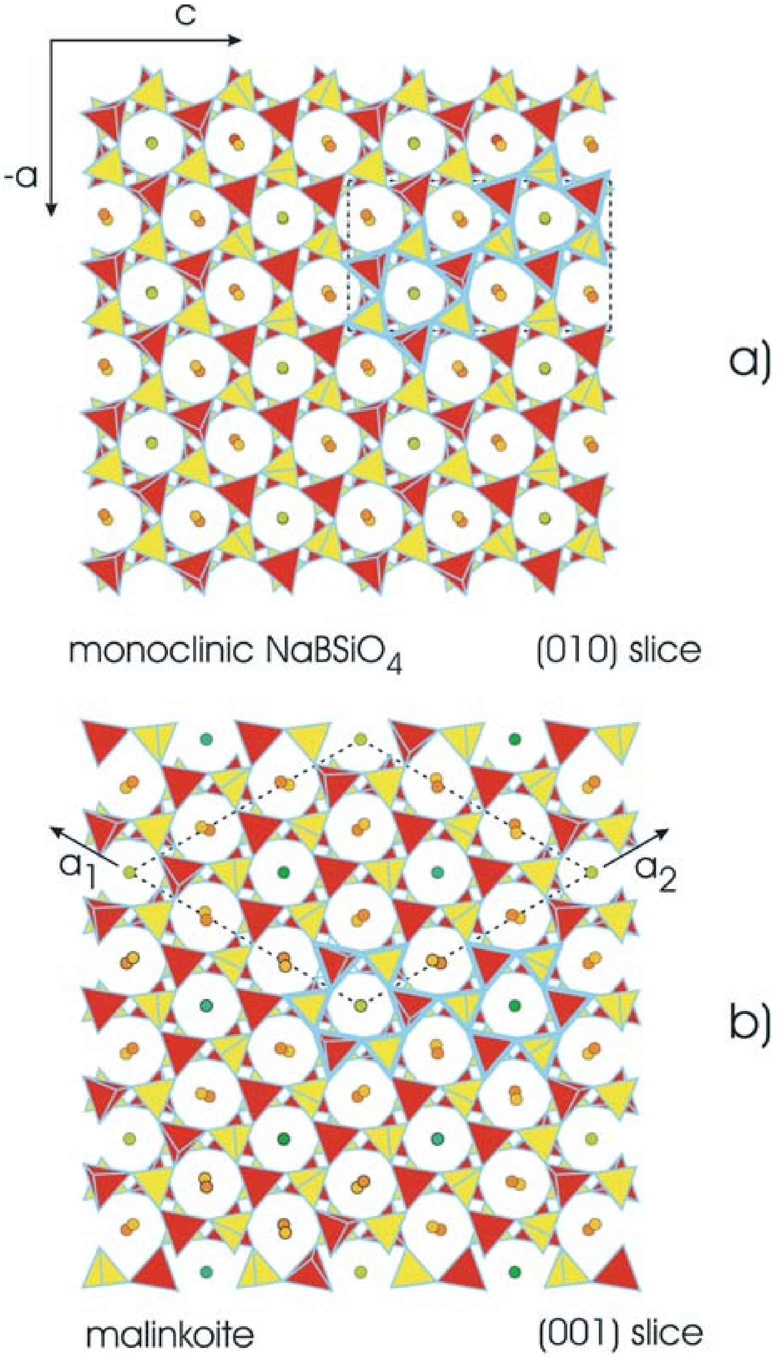

FIG. 2. Polyhedral model of monoclinic $NaBSiO_4$ and hexagonal malinkoite. SiO_4 tetrahedra are colored red, and BO_4 tetrahedra, yellow. The stuffing sodium atoms are displayed as circles (not to scale): green for nine-coordinated and yellow or brown for six-coordinated sodium. Two tridymite-like *UDUDUD* six-membered rings of tetrahedra with different orientations are drawn with bold lines. The structural data for malinkoite were taken from Sokolova *et al*. (2001). The unit cells are outlined by dashed lines.

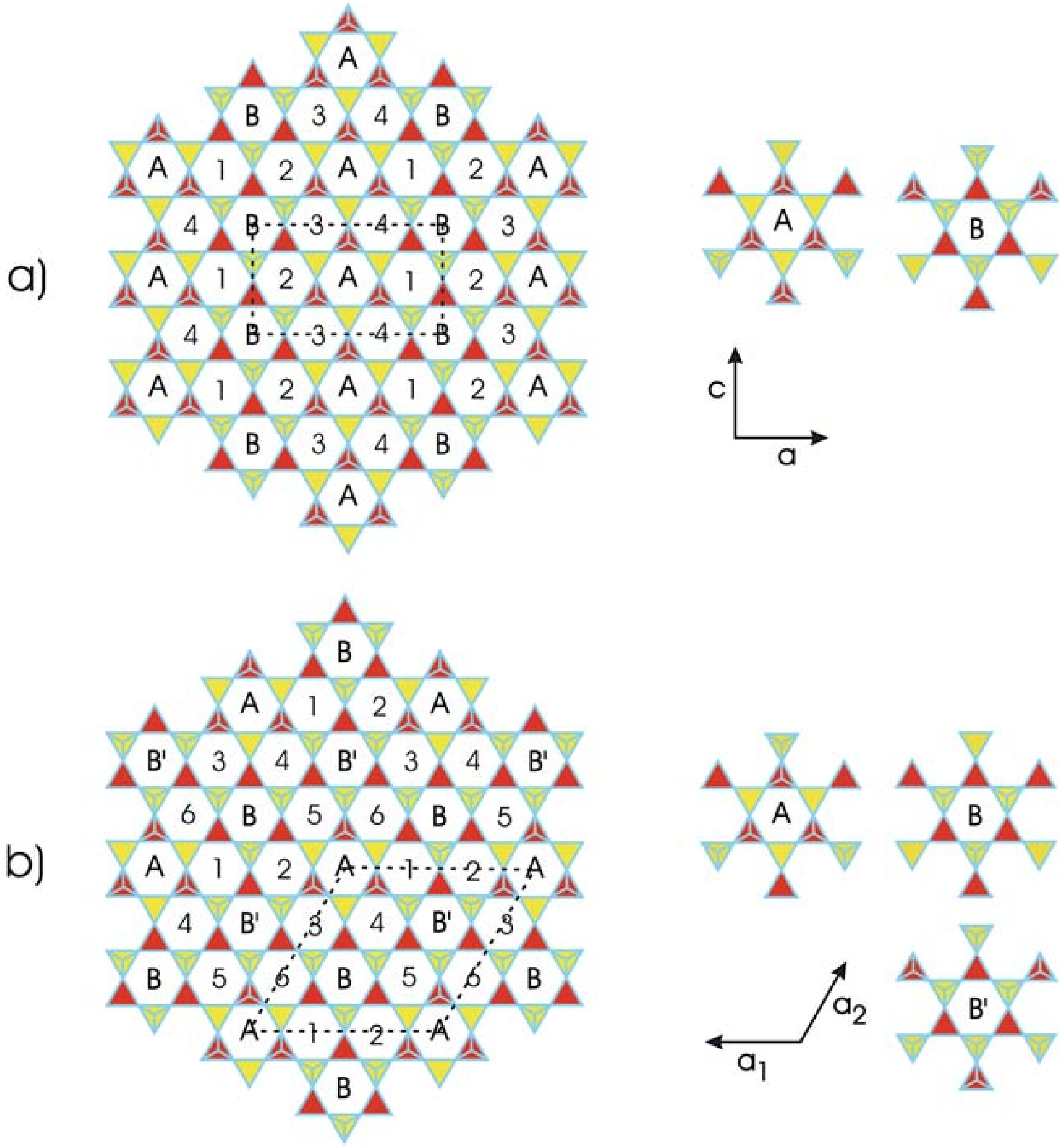

FIG. 3. Schematic drawing of two layers made up of one third *UDUDUD* and two thirds of *UUDDUD* rings, a) beryllonite and b) malinkoite. The SiO$_4$ tetrahedra are colored red, and the BO$_4$ tetrahedra, yellow. *A* and *B* (*B'*) denote different orientations of tridymite-like *UDUDUD* rings, *B'* has a different surrounding of next-nearest tetrahedra compared to *B,* as indicated on the right side. The unit cells are outlined by dashed lines. The numbers depict four (in a) and six (in b) different orientations of the *UUDDUD* rings (see text).

nepheline and kalsilite exclusively contain six-membered rings of tetrahedra whose apices point in alternate direction, up (*U*) and down (*D*), when viewed along the hexagonal or pseudohexagonal axis. In both monoclinic $NaBSiO_4$ (with the beryllonite structure) and malinkoite (Sokolova *et al.* 2001), only one third of the rings is of this *UDUDUD* type, whereas two thirds of the rings are of the *UUDDUD* type, with two pairs of adjacent tetrahedra per ring pointing in the same direction (Figs. 2a, b, 3). Both types of rings are distorted in a similar way to a trigonal shape by twisting of the tetrahedra in both monoclinic and hexagonal $NaBSiO_4$. The twisting is slightly stronger for the smaller (BO_4) tetrahedra than for the (SiO_4) tetrahedra (Figs. 2a, b). The main difference in the frameworks of tetrahedra in the two phases lies in the way in which the two different rings are linked (*cf.* Sokolova *et al.* 2001). The different linkages of these rings exclude the possibility of a simple displacive transformation between monoclinic and hexagonal $NaBSiO_4$; a phase transition would require rupture and reconstruction of bonds.

The combination of the two types of rings leads to a virtually infinite number of possibilities in the way the rings can be connected to a three-dimensional framework (Smith 1977). Thus, additional polymorphs of $NaBSiO_4$ are possible, in principle. The topology of two variants with one third *UDUDUD* and two thirds *UUDDUD* rings having the smallest possible set of lattice parameters has been outlined by Smith (1977). One of them corresponds to the beryllonite structure, and the other, to malinkoite.

The tridymite-like *UDUDUD* rings occur in two different orientations (labeled *A* and *B* in Fig. 3). As a consequence of the alternating distribution of cations over the tetrahedra in $NaBSiO_4$, all three *U* tetrahedra are either occupied by silicon or by boron (for *A* and *B* orientations, respectively). *UDUDUD* rings with different orientations can be connected in various ways (Fig. 3). Each *UDUDUD* ring is always surrounded by six *UUDDUD* rings. The simplest pattern (Fig. 3a) corresponds to the topology of beryllonite. The unit cell contains one *UDUDUD* ring in *A* orientation and one in *B* orientation. The *UUDDUD* rings occur in four different orientations (labeled 1 to 4 in Fig. 3a).

TABLE 2. ATOM COORDINATES FOR MONOCLINIC $NaBSiO_4$

Atom	*x*	*y*	*z*
Si1	0.9212(12)	0.7885(14)	0.2376(7)
Si2	0.1074(13)	0.2923(12)	0.0796(8)
Si3	0.4320(13)	0.7927(12)	0.0921(7)
Na1	0.245(2)	0.010(3)	0.250(2)
Na2	0.734(3)	0.470(3)	0.0802(19)
Na3	0.775(3)	0.032(3)	0.0662(15)
B1	-0.0774(13)	0.1677(14)	0.2383(7)
B2	0.1017(13)	0.6707(13)	0.0807(8)
B3	0.5655(15)	0.8287(13)	-0.0899(8)
O1	0.0652(18)	0.766(2)	0.3187(9)
O2	0.0573(18)	0.265(2)	0.1911(9)
O3	0.2378(14)	0.773(2)	0.1241(10)
O4	0.7400(15)	0.747(2)	0.2844(11)
O5	-0.0513(17)	0.249(2)	0.0108(10)
O6	0.452(2)	0.744(2)	-0.0206(7)
O7	0.9579(18)	0.664(2)	0.1466(11)
O8	0.2633(15)	0.169(2)	0.0509(12)
O9	0.550(2)	0.669(2)	0.1572(8)
O10	0.924(2)	0.9885(14)	0.2015(10)
O11	0.163(2)	0.4930(12)	0.0639(14)
O12	0.4899(19)	0.9922(12)	0.1093(16)

Overall isotropic displacement-parameter *U*iso = 0.0137(17).

The topology of malinkoite is more complicated (Fig. 3b). The unit cell is larger and contains one *UDUDUD* ring in the *A* orientation and two in the *B* orientation. The two rings in the *B* orientation differ in the configuration of the next-nearest tetrahedra. For one of them, all the next-nearest tetrahedra point downward, and for the other, upward (labeled as *B* and *B'* in Fig. 3b, respectively). Six different orientations of the *UUDDUD* rings can be distinguished here (labeled as 1 to 6 in Fig. 3b).

The stuffing atoms

The sodium ions occupy interstices within the tunnels of the structure of both monoclinic $NaBSiO_4$ and malinkoite. The boundaries of the tunnels are formed by the six-membered rings of tetrahedra. The coordinating atoms of oxygen form either distorted octahedra or an even more irregular nine-fold coordination depending on whether the sodium atoms are located in *UUDDUD* or *UDUDUD* rings, respectively (Figs. 2, 4).

Within the tridymite-like *UDUDUD* rings, the nine-fold coordinated sodium atoms are approximately centered in the middle of the rings forming chains running parallel to the *b* axis of monoclinic (pseudohexagonal) $NaBSiO_4$ (Figs. 2a, 4c) and parallel to the *c* axis in the hexagonal malinkoite (Figs. 2b, 4d). The nine interatomic Na–O distances cover a range from 2.53 to 2.77 Å in monoclinic $NaBSiO_4$. The six nearest atoms of oxygen form an approximately trigonal antiprism whose equator is surrounded by three further oxygen atoms. A second coordination-sphere is formed by three additional atoms of oxygen at distances of 2.96, 3.02 and 3.04 Å. In malinkoite, where the sodium atoms lie on special positions, the coordination is more regular, with three sets of equal Na–O distances ranging from 2.55 to 2.80 Å (Sokolova *et al.* 2001). The interatomic distances and angles of monoclinic $NaBSiO_4$ are listed in Table 3.

Within the *UUDDUD* rings, the distorted NaO_6 octahedra form pairs by sharing a common face. The pairs of octahedra are separated in the direction of the tunnel axis by an unoccupied site (Figs. 4c, d). Viewed along the *b* axis of monoclinic (pseudohexagonal) $NaBSiO_4$ and the *c* axis of the hexagonal malinkoite, the sodium atoms are displaced from the middle of the *UUDDUD* rings. Whereas there is only one direction for the alternating displacements in monoclinic $NaBSiO_4$ (Fig. 2a), malinkoite has three directions for the displacements according to the higher symmetry and different orientations of the UUDDUD rings (Fig. 2b).

DISCUSSION

From the published data, it seems likely that the crystal structure of synthetic monoclinic NaBSiO$_4$ is identical with that of the unnamed mineral UK53. There is, however, one further unnamed NaBSiO$_4$ mineral with hexagonal symmetry labeled as UK53B and reported to occur at Mont Saint-Hilaire as well (Wight & Chao 1995). This might be a candidate for a further polymorph. Whereas mineral UK53A is identical with malinkoite (pers. commun., E. Sokolova, 2004), no further data are available for UK53B.

Monoclinic NaBSiO$_4$ has the smallest unit-cell volume of all known monoclinic beryllonite-type (*sensu stricto*) compounds, characterized by a moderate size of the stuffing ions Na$^+$ or Ca^{2+}, and only a little K$^+$ (Fig. 5). For aluminosilicates, larger cations like K$^+$ require other stuffed derivatives of the tridymite framework, such as kalsilite or kaliophilite, KAlSiO$_4$. Smaller stuffing cations, like Li$^+$, on the other hand, lead to the β-eucryptite (stuffed high-quartz) and phenakite structure types (Liebau 1985).

The unit-cell volume of NaTT'O$_4$ with T = B, Al and Ga and T' = Si and Ge varies linearly with the size of the framework cations (Fig. 5). Polymorphism is well known (*e.g.*, NaAlSiO$_4$ crystallizes with the beryllonite, carnegieite and nepheline structures). Apart from NaBSiO$_4$, the malinkoite structure has not been observed for the other compounds that show a stuffed derivative structure of tridymite. The calculated densities, 2.926 and 2.922 g/cm^3 for monoclinic and hexagonal NaBSiO$_4$, respectively, [measured densities: 2.86 g/cm^3 for UK53 (Chao *et al.* 1990) and 2.85(2) g/cm^3 for malinkoite (Sokolova *et al.* 2001)] do not differ significantly, and do not allow any conclusions as to the relative stability of the two polymorphs. The synthesis shows that monoclinic NaBSiO$_4$ may be stable at high pressures, but its probable occurrence in the subvolcanic environment of Mont Saint-Hilaire suggests an extended range of stability to low pressures as well. Moreover, small chemical differences (impurities) may play a role. More experimental work on NaBSiO$_4$ under varying pressures and temperatures is required.

TABLE 3. INTERATOMIC DISTANCES (Å) AND ANGLES (°) OF MONOCLINIC NaBSiO$_4$

Na1-O3^{1}	2.53(3)	Na2-O11^{6}	2.19(3)	Na3-O10^{1}	2.25(3)
Na1-O1^{2}	2.55(3)	Na2-O6^{6}	2.37(3)	Na3-O8^{8}	2.27(3)
Na1-O2^{3}	2.59(3)	Na2-O9	2.38(3)	Na3-O5^{8}	2.30(3)
Na1-O2	2.61(3)	Na2-O7	2.50(3)	Na3-O12^{1}	2.38(3)
Na1-O10^{4}	2.66(2)	Na2-O4^{7}	2.56(3)	Na3-O6^{6}	2.58(3)
Na1-O1^{5}	2.67(3)	Na2-O5^{8}	2.60(3)	Na3-O4^{7}	2.66(3)
Na1-O3^{3}	2.68(3)				
Na1-O11^{3}	2.70(3)	*<Na2-O>*	2.43	*<Na3-O>*	2.41
Na1-O12^{1}	2.77(3)				
<Na1-O>	2.64				
Si1-B1^{6}	2.908(12)	Si2-B1	2.832(11)	Si3-B1^{9}	2.804(11)
Si1-B1^{9}	2.932(12)	Si2-B2	2.905(10)	Si3-B2	2.805(11)
Si1-B2^{8}	2.778(12)	Si2-B2^{11}	2.801(12)	Si3-B3	2.765(12)
Si1-B3^{10}	2.819(12)	Si2-B3^{6}	2.774(12)	Si3-B3^{12}	2.909(9)
<Si1-B>	2.859	*<Si2-B>*	2.828	*<Si3-B>*	2.821
Si1^{13}-O1-B3^{14}	131.1(12)	Si2-O2-B1	132.7(11)	Si3-O3-B2	130.1(12)
Si1-O4-B1^{9}	141.6(12)	Si2-O5-B2^{11}	129.6(13)	Si3-O6-B3	126.5(13)
Si1-O7-B2^{8}	127.6(11)	Si2-O8-B3^{6}	128.0(12)	Si3-O9-B1^{9}	130.1(11)
Si1-O10-B1^{6}	141.4(11)	Si2-O11-B2	140.5(14)	Si3-O12-B3^{12}	140.7(13)
<Si1-O-B>	135.4	*<Si2-O-B>*	132.7	*<Si3-O-B>*	131.9

Si–O and B–O distances were constrained to be 1.62 Å and 1.47 Å, respectively, and the O–T–O angles, to be 109.5°.

1) – x, – 1 – y, – z; 2) x, – 1 + y, z; 3) 1/2 + x, – 1/2 – y,1/2 + z; 4) – 1 – x, – 1 – y, – z; 5) 1/2 – x, 1/2 + y, 1/2 – z; 6) 1 – x, 1 – y, – z; 7) 3/2 + x, – 1/2 – y, 1/2 + z; 8) 1 – x, – y, – z; 9) 1/2 + x, 1/2 – y, 1/2 + z; 10) 1 – x, 2 – y, – z; 11) – x, 1 – y, – z; 12) 1/2 + x, 3/2 – y, 1/2 + z; 13) – 1 + x, y, z; 14) – 1/2 + x, 3/2 – y, 1/2 + z.

ACKNOWLEDGEMENTS

We thank Mark Ufer for the preparation and preliminary characterization of the NaBSiO$_4$ sample and Elena V. Sokolova, Jeffrey E. Post and Dana T. Griffen for their thorough reviews and critical comments.

REFERENCES

BARBIER, J. & FLEET, M.E. (1987): Investigation of structural states in the series *M*GaSiO$_4$, *M*AlGeO$_4$, *M*GaGeO$_4$ (M = Na, K). *J. Solid State Chem.* **71**, 361-370.

CHAO, G.Y., CONLON, R.P. & VAN VELTHUIZEN, J. (1990): Mont Saint-Hilaire unknowns. *Mineral. Rec.* **21**, 363-368.

GOLOVASTIKOV, N.I. (1962): The crystal structure of beryllonite (NaBePO$_4$). *Sov. Phys. Crystallogr.* **6**, 733-739.

HENDERSON, C.M.B. & TAYLOR, D. (1984): Thermal expansion behaviour of beryllonite [Na(BePO$_4$)] and trimerite [CaMn(BeSiO$_4$)$_3$]. *Mineral. Mag.* **48**, 431-436.

KLASKA, R., KLASKA, K.-H. & JARCHOW, O. (1979): Struktur und Verwachsung zweier topologisch unterschiedlicher Tetraedergerüste der Pseudosymmetrie *Icmm. Z. Kristallogr.* **149**, 135-137.

LEBAIL, A., DUROY, H. & FOURQUET J.L. (1988): Ab initio structure determination of LiSbWO$_4$ by X-ray powder diffraction. *Mater. Res. Bull.* **23**, 447-452.

LIEBAU, F. (1985): *Structural Chemistry of Silicates. Structure, Bonding and Classification*. Springer-Verlag, Berlin, Germany.

PETRICEK, V. & DUSEK, M. (2003): *Jana2000. Crystallographic Computing System.* Institute of Physics, Academy of Science, Praha, Czech Republic. http://www-xray.fzu.cz/jana/jana-html

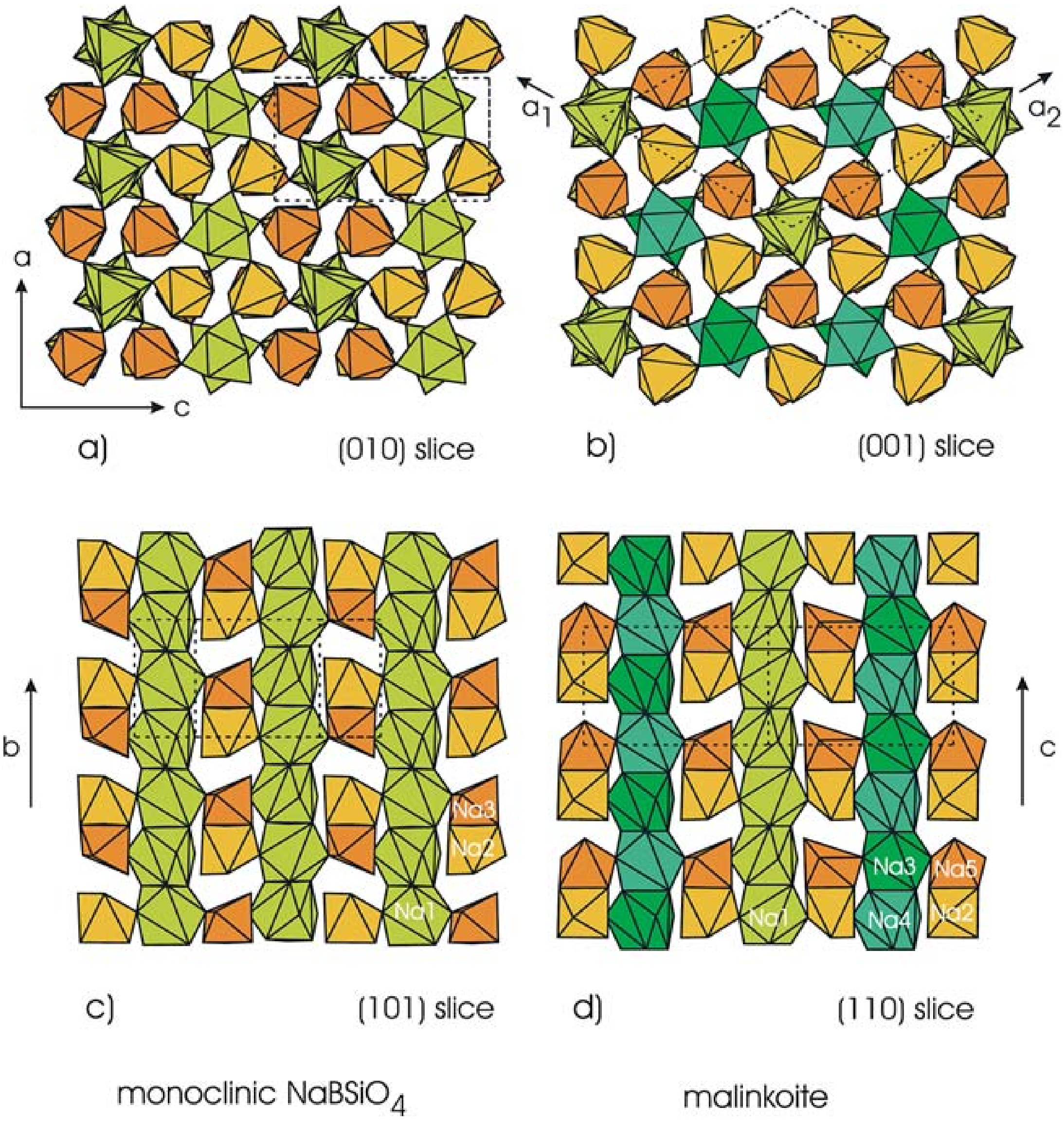

FIG. 4. Polyhedral model of the first coordination sphere of the sodium atoms. Left side: in beryllonite-type $NaBSiO_4$, right side: in malinkoite. The nine-fold coordination in the tridymite-like *UDUDUD* rings is shown in various shades of green, and the octahedra within the *UUDDUD* rings are brown and yellow. The structural data for malinkoite were taken from Sokolova *et al.* (2001). The unit cells are outlined by dashed lines.

SANDOMIRSKII, P.A., MESHALKIN, S.S., ROZHDESTVENSKAYA, I.V., DEM'YANETS, L.N. & UVAROVA, T.G. (1986): Crystal structures of the *D*-phase of K{$AlGeO_4$} and the *C*-phase Na{$AlGeO_4$}. *Sov. Phys. Crystallogr.* **31**, 522-527.

SCHREYER, W. & WERDING, G. (1997): High-pressure behaviour of selected boron minerals and the question of boron distribution between fluids and rocks. *Lithos* **41**, 251-266.

SHANNON, R.D. (1976): Revised effective ionic radii and systematic studies of interatomic distances in halides and chalcogenides. *Acta Crystallogr.* **A32**, 751-767.

SMITH, J.V. (1977): Enumeration of 4-connected 3-dimensional nets and classification of framework silicates. I. Perpendicular linkage from simple hexagonal net. *Am. Mineral.* **62**, 703-709.

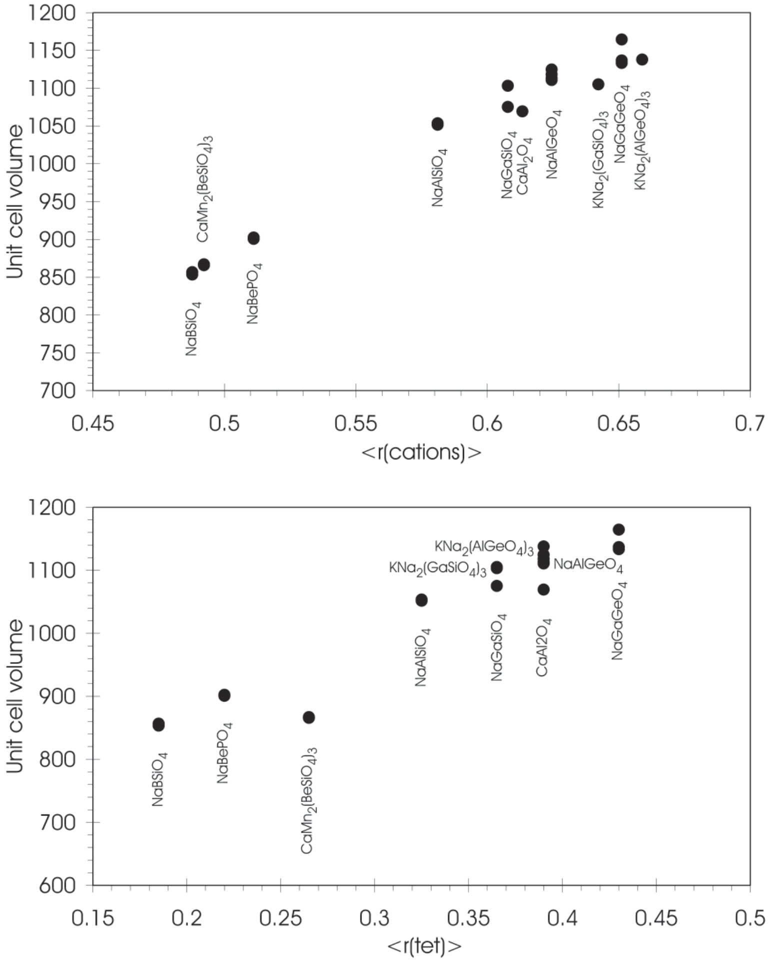

FIG. 5. Unit-cell volume of $ATT'O_4$ compounds with the monoclinic structure of beryllonite *versus* (a) the average radius of the cations, and (b) the average radius of the tetrahedrally coordinated cations. The lattice parameters were taken from Klaska *et al.* (1979), Henderson & Taylor (1984), Sandomirskii *et al.* (1986), Barbier & Fleet (1987), and the effective ionic radii, from Shannon (1976).

SOKOLOVA, E.V., HAWTHORNE, F.C. & KHOMYAKOV, A.P. (2001): The crystal chemistry of malinkoite, $NaBSiO_4$, and lisitsynite, $KBSi_2O_6$, from the Khibina–Lovozero complex, Kola Peninsula, Russia. *Can. Mineral.* **39**, 159-169.

UFER, M. (1996): *Synthese und Stabilität von Reedmergnerit im System $Na_2O - B_2O_3 - SiO_2 - H_2O$.* Diplomarbeit am Institut für Mineralogie der Ruhr-Universität Bochum, Germany

________ & SCHREYER, W. (1996): Synthese und Druckstabilität des "Bor-Albits" Reedmergnerit. *Ber. Deutsch. Mineral. Gesellschaft* **8**, 292 (abstr.).

WERDING, G. & SCHREYER, W. (1996): Experimental studies on borosilicates and selected borates. *In* Boron: Mineralogy, Petrology and Geochemistry (E.S. Grew & L.M. Anovitz, eds.). *Rev. Mineral.* **33**, 117-163.

WIGHT, Q. & CHAO, G.Y. (1995): Mont Saint-Hilaire, revisited; part 2. *Rocks & Minerals* **70**, 90-103 and 131-138.

Received July 22, 2004, revised manuscript accepted January 19, 2005.